

# 1

## Neural Dynamics: Criticality, Cooperation, Avalanches and Entrainment between Complex Networks

*P. Grigolini, M. Zare, A. Svenkeson, B. J. West*

### 1.1

#### Introduction

The discovery of avalanches in neural systems [1] has aroused substantial interest among neurophysiologists and, more generally, among researchers in complex networks [2] as well. The main purpose of this chapter is to provide evidence in support of the hypothesis that the phenomenon of *neural avalanches* [1] is generated by the same cooperative properties as those responsible for a surprising effect that we call *cooperation-induced* synchronization, illustrated in [3]. The phenomenon of neural entrainment [4] is another manifestation of the same cooperative property. We also address the important issue of the connection between neural avalanches and *criticality*. Avalanches are thought to be a manifestation of criticality, and especially self-organized criticality [5, 6]. At the same time, criticality is accompanied by long-range correlation [5] and a plausible model for neural dynamics is expected to account for the astounding interaction between agents separated by relatively large distances. General agreement exists in the literature that brain function rests on these crucial properties, and the phase transition theory for physical phenomena [7] is thought to afford the most important theoretical direction for further research work on this subject. In this theory criticality emerges at a specific single value of a control parameter, designated by the symbol  $K_c$ . In this chapter we illustrate a theoretical model generating avalanches, long-range correlation and entrainment, as a form of cooperation-induced synchronization, over a wide range of values of the control parameter  $K$ , thereby suggesting that the form of criticality within the brain is not the ordinary criticality of physical phase transitions but is instead the *extended criticality* recently introduced by Longo and co-workers [8] to explain biological processes.

Cooperation is the common effort of the elements of a network for their mutual benefit. We use the term cooperation in the same loose sense as that adopted, for instance, by Montroll [9] to shed light on the equilibrium condition realized by the interacting spins of the Ising model. Although the term cooperation, frequently used in this chapter, does not imply a network's cognition, we follow the conceptual

perspective advocated by Werner [10] that cognition emerges at criticality, with the proviso that its cause may be extended criticality.

The term *cooperation* suggests a form of awareness that these units do not have and must be used with caution especially because in this chapter we move from an Ising-like model to a model of interacting neurons that seems to reproduce certain experimental observations on neural networks that are thought to reflect important properties of brain dynamics, including the emergence of cognition. This is done along the lines advocated by Werner [10], who argues that consciousness is a phenomenon of statistical physics resting on renormalization group theory [11]. We afford additional support to this perspective, while suggesting that the form of criticality from which cognition emerges may be more complex than renormalization group criticality, thereby requiring an extension of this theory. All this must be carried out keeping in mind Werner's warning [12] against the use of metaphors of Computation and Information, which would contaminate the observation with meanings from the observer's mind.

We move from an Ising-like cooperative model to one of interacting neurons that, although highly idealized, serves very well the purpose of illustrating the cooperative-induced temporal complexity of neural networks. The reason to spend time with the Ising-like cooperative model, discussed in this Volume by West *et al.* [3], is the fact that dealing first with this model clarifies the difference between ordinary criticality, shared with this earlier model, and extended criticality.

The Ising-like model that we adopt is the decision making model (DMM) that has been used to explain the scale-free distribution of neural links recently revealed by the fMRI analysis of the brain [13, 14]. We examine two different weak-perturbation conditions: (i) all the units are perturbed by an external low-intensity stimulus; (ii) a small number of units are perturbed by an external field of large intensity. We show that the response of this cooperative network to extremely weak stimuli, case (i), departs from the predictions of traditional linear response theory (LRT) originally established by Green and Kubo [15] and widely applied by physicists for almost 60 years. This deviation arises because cooperation generates phase transition criticality and at the same time it generates non-ergodic fluctuations, whereas the traditional LRT is confined to the condition of ergodic fluctuations. Condition (ii) is the source of another surprising property: although a few units are strongly perturbed, thanks to cooperation the stimulus affects the whole network, making that response depart from either ergodic or non-ergodic LRT, thereby generating what we call *cooperation-induced* (CI) response. This form of response is the source of perfect synchronization between a complex network and the perturbing stimulus generated by another complex network, a new phenomenon discovered by Turalska *et al* [16] whose cooperative origin is illustrated in detail in this Chapter. We term this effect CI synchronization. Condition (i) yields the non-ergodic extension of stochastic resonance, and the CI synchronization of condition (ii) is the cooperative counterpart of chaos synchronization.

The second step of our approach to understanding neural complexity and neural avalanches [17] rests on an *integrate and fire* model [18] where the firing of one unit of a set of linked neurons facilitates the firing of the other units. We

refer to this model as Neural Firing Cooperation (NFC). We find that in the case where cooperation is established through NFC the emerging form of criticality is significantly different from that of an ordinary phase transition. In the typical case of phase transition temporal complexity is limited to a singular value of the control parameter, namely, of the cooperation strength in the cases examined in this chapter. The NFC cooperation generates temporal complexity analogous to that generated by the DMM, but this temporal complexity, rather than being limited to a single value of the cooperation parameter, is extended to a finite interval of critical values. As a consequence, the new ways of responding to external stimuli are not limited to a singular value of the cooperation parameter either, but their regime of validity is significantly extended suggesting this to be a manifestation of the new form of criticality that Longo and co-workers [8] call *extended criticality* (EC). Adopting the EC perspective we move within the extended critical range, from smaller to larger values of the cooperation parameter  $K$ , and we find that neural avalanches [17] emerge at the cooperation level making the system adopt the CI response. When a neural network is driven by another neural network with the same complexity, we expect that the response of the perturbed network obeys the new phenomenon of CI synchronization. We notice that these theoretical predictions, of a close connection to neural avalanches and network entrainment, can be checked experimentally through methods of the kind successfully adopted in the University of North Texas laboratory of G.W. Gross [19].

Finally, although the emergence of consciousness remains a mystery, we note that the assignment of cognition properties to cooperation [20] leads to temporal complexity with the same power-law index as that revealed by the experimental observation of active cognition [21], thereby supporting the conjecture [11] that a close connection between cognition in action and a special form of temporal complexity exists.

The connection between neural cooperation and cognition is certainly far beyond our current understanding of emerging consciousness. Therefore, we limit ourselves to showing that the cooperation between units generates global properties, some of which are qualitatively similar to those revealed by recent analysis of the human brain.

## 1.2

### Decision Making Model (DMM) at Criticality

The DMM [16] is the Ising-like version of an earlier model [22] of a dynamic complex network. The DMM is based on the cooperative interaction of  $N$  units, each of which is described by the master equation

$$\frac{d}{dt}p_1^{(i)}(t) = -\frac{g_{12}^{(i)}(t)}{2}p_1^{(i)}(t) + \frac{g_{21}^{(i)}(t)}{2}p_2^{(i)}(t) \quad (1.1)$$

$$\frac{d}{dt}p_2^{(i)}(t) = -\frac{g_{21}^{(i)}(t)}{2}p_2^{(i)}(t) + \frac{g_{12}^{(i)}(t)}{2}p_1^{(i)}(t), \quad (1.2)$$

where

$$g_{12}^{(i)} \equiv g_0 \exp\left(K \frac{(N_2^{(i)} - N_1^{(i)})}{N^{(i)}}\right) \quad (1.3)$$

and

$$g_{21}^{(i)} \equiv g_0 \exp\left(K \frac{(N_1^{(i)} - N_2^{(i)})}{N^{(i)}}\right). \quad (1.4)$$

The symbol  $N^{(i)}$  denotes the number of nodes linked to the  $i$ -th node, with  $N_1^{(i)}$  and  $N_2^{(i)}$  being those in the first and second state, respectively. Of course,  $N^{(i)} = N_1^{(i)} + N_2^{(i)}$ .

The index  $i$  runs from 1 to  $N$ , where  $N$  is the total number of nodes of the complex network under study, thereby implying that we have to compute  $N$  pairs of equations of the kind of Eqs. (1.1) and (1.2) at each time step. The adoption of an all-to-all coupling condition allows us to simplify the problem. In fact, in that case all the  $N$  pairs of equations are identical to

$$\frac{d}{dt}p_1(t) = -\frac{g_{12}(t)}{2}p_1(t) + \frac{g_{21}(t)}{2}p_2(t) \quad (1.5)$$

$$\frac{d}{dt}p_2(t) = -\frac{g_{21}(t)}{2}p_2(t) + \frac{g_{12}(t)}{2}p_1(t), \quad (1.6)$$

with

$$g_{12} \equiv g_0 \exp\left(K \frac{(N_2 - N_1)}{N}\right) \quad (1.7)$$

and

$$g_{21} \equiv g_0 \exp\left(K \frac{(N_1 - N_2)}{N}\right). \quad (1.8)$$

Since normalization requires  $p_1(t) + p_2(t) = 1$ , it is convenient to replace the pair of Eqs. (1.5) and (1.6) with a single equation for the difference in probabilities

$$\Pi(t) \equiv p_1(t) - p_2(t), \quad (1.9)$$

which after some simple algebra becomes

$$\frac{d}{dt}\Pi = \frac{(g_{21} - g_{12})}{2} - \frac{(g_{21} + g_{12})}{2}\Pi. \quad (1.10)$$

It is important to stress that the equality

$$\frac{N_1 - N_2}{N} = \Pi \quad (1.11)$$

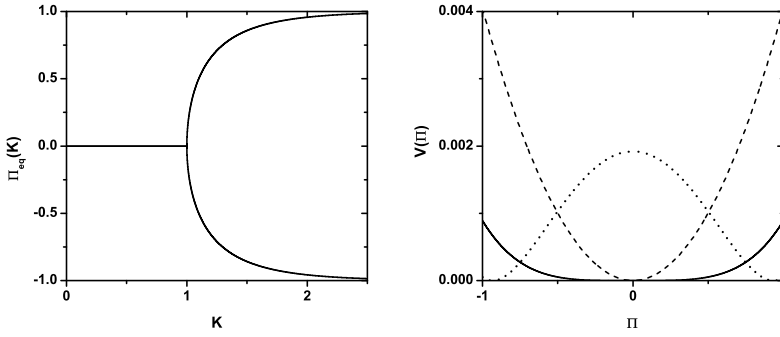


**Figure 1.1** (Left panel) The equilibrium mean field for different values of the cooperation parameter  $K$ . A bifurcation occurs at the critical point  $K = K_c = 1$ . (Right panel) Potential barriers for  $K$  subcritical (dashed line,  $K = 0.2$ ), critical (solid line,  $K = 1.0$ ), and supercritical (dotted line,  $K = 1.8$ ).

holds true only in the limiting case  $N \rightarrow \infty$ . In the case of a finite network,  $N < \infty$ , the mean field fluctuates in time forcing us to adopt

$$\frac{N_1 - N_2}{N} = \Pi + f(t), \quad (1.12)$$

where  $f(t)$  is a random fluctuation, which according to the Law of Large Numbers has an intensity proportional to  $1/\sqrt{N}$ . Inserting Eq. (1.12) into Eq. (1.10) yields

$$\frac{d}{dt}\Pi = \frac{g_0}{2} \left( e^{K\Pi} e^{Kf} - e^{-K\Pi} e^{-Kf} \right) - \frac{g_0}{2} \left( e^{K\Pi} e^{Kf} + e^{-K\Pi} e^{-Kf} \right) \Pi \quad (1.13)$$

and in the limiting case  $N \rightarrow \infty$  the fluctuations vanish,  $f = 0$ , so that Eq. (1.13) generates the well known phase transition prediction at the critical value of the control parameter

$$K_c = 1. \quad (1.14)$$

Fig. 1.1 shows that for  $K \leq 1$  the mean field has only one possible equilibrium value,  $\Pi_{eq} = 0$ . At the critical point  $K = K_c = 1$  this vanishing equilibrium value splits into two opposite components, one positive and one negative. To understand the important role of criticality, we notice that a finite number of units generates the fluctuation  $f$  and, this, in turn, forces fluctuations in the mean field. At criticality, the fluctuations induced in  $\Pi(t)$  have a relatively extended range of free evolution, as made clear in Fig. 1.1. In fact, the separation between the two repulsive walls is greatest at criticality. In between them, a free diffusion regime occurs. The supercritical condition  $K > K_c$  generates a barrier of higher and higher intensity with the increase of  $K$ . At the same time the widths of the two wells shrink, bounding the free evolution regime of the fluctuating mean field to a smaller region.

## 1.2.1

**Intermittency**

Considering a large but finite number of units and expanding Eq. (1.13) to the lowest order contributions of  $\Pi$  and  $f$ , it is straightforward to prove that for either  $K > 1$  or  $K < 1$ , due to conditions illustrated in Fig. 1.1, the mean field fluctuations are driven by an ordinary Langevin equation of the form

$$\frac{d}{dt}x = -\Gamma x + \xi(t). \quad (1.15)$$

Note that when  $K > 1$ ,

$$x(t) \equiv \Pi(t) - \Pi_{eq}(K), \quad (1.16)$$

where  $\Pi_{eq}(K)$  denotes the equilibrium value for  $N = \infty$ . Of course, at either criticality or in the subcritical condition  $\Pi_{eq}(K) = 0$ , thereby making  $x(t)$  coincide with  $\Pi(t)$ .

At the critical point  $K = K_c = 1$ , we find the time evolution of the mean field to be described by a nonlinear Langevin equation of the form

$$\frac{d}{dt}x = -\gamma x^3 + \xi(t). \quad (1.17)$$

The linear term that dominates in Eq. (1.15) vanishes identically, and the cooperation between units at criticality displays a remarkable change in behavior which is characterized by the weakly repulsive walls of Fig. 1.1.

If we interpret the conditions  $x > 0$  and  $x < 0$  as corresponding to the light and dark states of blinking quantum dots [23] the DMM provides a satisfactory theoretical representation of this complex intermittent process. It was, in fact noticed [23] that if the survival probability  $\Psi(t)$ , namely the probability that a given state, either light or dark, survives for a time  $t$  after its birth, is evaluated beginning its observation at a time distance  $t_a$  from its birth, then its decay becomes slower (aging). Furthermore, this aging effect is not affected by randomly time-ordering the sequence of light and dark states. Notice that the aged curves of Fig. 1.2 are actually doublets of survival probabilities generated by shuffled and non-shuffled sequences of states, thereby confirming the renewal nature of this process.

Fig. 1.2 shows that the inverse power law region of the survival probability, corresponding to an inverse power law waiting time distribution density with power law index  $\mu = 1.5$ , has a limited time range of validity. This limitation arises because Eq. (1.17) has an equilibrium distribution, generated by the confining action of the friction term. Thus, the upper time limit of the inverse power law waiting time distribution density is determined by the relation  $t < T_{eq}$  with

$$T_{eq} \approx \left( \frac{1}{\gamma D} \right)^{1/2} \quad (1.18)$$

where the diffusion coefficient  $D$  is proportional to  $1/N$ . This theoretical prediction is obtained by means of straightforward dimensional arguments [24].

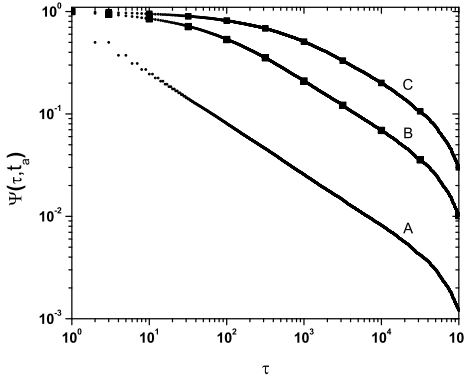


**Figure 1.2** The  $t_a$ -aged survival probability of the mean field fluctuations  $x$  at criticality  $K = 1$  for  $N = 1000$  units and  $g_0 = 0.01$ . (A)  $t_a = 0$ , power index  $\mu - 1 = 0.5$ . (B)  $t_a = 100$ . (C)  $t_a = 1000$ . The squares in (B) and (C) correspond to the  $t_a$ -aged survival probability of randomly shuffled sequences of waiting times. Their equivalence to the non-shuffled aged survival probability indicates the fluctuations are renewal.

Notice that in the traditional case of the ordinary Langevin equation, the restoring term  $-\gamma x^3$  of Eq. (1.17) is replaced by  $-\gamma x$  and  $T_{eq} \approx 1/\gamma$ , implying that at criticality the transient regime is  $(\gamma/D)^{1/2}$  times larger than the conventional transition to equilibrium. Remember that we have assumed the number of interacting units to be large but finite, thereby generating small fluctuations under the condition  $D \ll \gamma$ . As a consequence, the temporal complexity illustrated in Fig. 1.2 becomes ostensible only at criticality, while remaining virtually invisible in both the subcritical and supercritical regimes.

Fig. 1.3 illustrates an important dynamical property of criticality concerning the fluctuations emerging as a finite-size effect. We have to stress that the fluctuations, bringing important information about the network's complexity, are defined by Eq. (1.16). We define the equilibrium autocorrelation function of the variate  $x$ ,  $\Phi(\tau)$ , as

$$\Phi(\tau) = \Phi(t, t') \equiv \frac{\langle x(t)x(t') \rangle}{\langle x^2 \rangle_{eq}}, \quad (1.19)$$

with the time difference

$$\tau \equiv t - t'. \quad (1.20)$$

Fig. 1.3 shows the important property that at criticality the equilibrium correlation function is markedly slower than in both the supercritical and the subcritical regimes. This property has to be kept in mind to appreciate the principal difference between ordinary and extended criticality. In fact, this is an indication that with ordinary criticality the significant effects of cooperation correspond to a single value of  $K$ , this being the critical value  $K = K_c = 1$ .

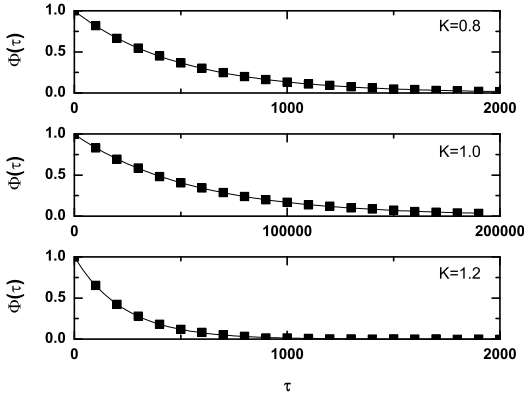


**Figure 1.3** The equilibrium correlation function for the fluctuations  $x$  in the subcritical (top panel), critical (middle panel), and supercritical (bottom panel) cases, each considering  $N = 1000$  units with  $g_0 = 0.01$ . The time scale of the exponential decay is increased by two orders of magnitude at criticality.

### 1.2.2

#### Response to perturbation

As far as the response to an external perturbation is concerned, it is important to address the issue of the connection with the phenomenon of complexity management [25]. We have noticed that at criticality, the fluctuation in sign  $\eta \equiv x/|x|$  is not ergodic for  $t < T_{eq}$ , thereby implying that the transmission of information from one network to another may require a treatment going beyond the traditional Green-Kubo approach. To recover the important results of Ref. [25] we should adopt a dichotomous representation fitting the nature of the DMM units that have to choose between the two states  $+$  and  $-$ . To simplify the numerical calculations, we assume that the influence of an external stimulus on the system is described by Eq. (1.21). This is a simplified picture that does not take into account that in the case of flocks of birds [26], for instance, the single units make a decision based on the  $+$  or  $-$  sign of the stimulus rather than on its actual value. In other words, in the case of flocks [26], this would imply that the external stimulus assigns to each bird either the right or the left direction.

The perturbed time evolution of the mean field at criticality is described by

$$\frac{d}{dt}x = -\gamma x^3 + \xi(t) + \epsilon\gamma F(t), \quad (1.21)$$

where  $F(t)$  is the external perturbation, and  $\epsilon$  a small dimensionless number that will serve the purpose of ensuring the linear response condition. The factor of  $\gamma$  is introduced for dimensional reasons.



We note that in the diffusional transient regime, which is much more extended in time than that generated by the traditional Langevin equation, Eq. (1.21) becomes

$$\frac{d}{dt}x(t) = \xi(t) + \epsilon\gamma F(t), \quad (1.22)$$

yielding the average response

$$\langle x(t) \rangle = \epsilon\gamma \int_0^t F(t') dt', \quad (1.23)$$

which, in the case where  $F(t) = A\cos(\omega t)$ , becomes

$$\langle x(t) \rangle = \frac{A\gamma\epsilon}{\omega} \sin(\omega t). \quad (1.24)$$

Taking into account that during the transient regime  $\langle x^2(t) \rangle = 2Dt$  we immediately obtain

$$\langle \eta(t) \rangle \propto \frac{1}{t^{0.5}} A\epsilon\gamma \sin(\omega t), \quad (1.25)$$

in accordance with the experimental observation [27] that the response of a non-ergodic system to harmonic perturbation generates damped oscillations.

The rigorous treatment would lead to

$$\langle \eta(t) \rangle = \epsilon\gamma \int_0^t d\tau \chi(t, \tau) F(\tau), \quad (1.26)$$

where

$$\chi(t, \tau) = -\frac{d}{dt} \Psi(t, \tau), \quad (1.27)$$

and  $\Psi(t, \tau)$  is the aged survival probability [24].

As a consequence we predict that at criticality the complex network obeys the principle of complexity management [25] when all the units are weakly perturbed by an external stimulus. The chapter of West *et al.* [3] in this volume shows that, due to cooperation, a strong perturbation on a limited number of units is the source of the related phenomenon of *cooperation-induced synchronization* that in this chapter we show to emerge also at the level of neural extended criticality, under the form of neural network entrainment.

### 1.3

#### Neural Dynamics

The cooperation of units within the DMM at criticality generates the temporal complexity illustrated by Fig. 1.2, which turns out to be a source of information transport. This transfer of information is especially convenient as shown in the recent work of Vanni *et al.* [26]. This cooperation property yields the surprising

effect of the crucial role of committed minorities discussed in this volume by West *et al.* [3].

In this section we illustrate a very similar property generated by a model of neurophysiological interest, with the surprising discovery that these effects do not rest on a single value of the cooperation strength, that is, on the magnitude of the control parameter. This suggests the conjecture that a new form of criticality, called extended may be invoked [8].

We show that the DMM leads to Plenz's avalanches [17], which are now a well established property of neural networks. The model proposed in this chapter interprets the avalanches as a manifestation of cooperation. We also show that the amount of cooperation generating avalanches is responsible for the phenomenon of entrainment.

### 1.3.1

#### Mittag-Leffler function models cooperation

First of all, let us examine how the Mittag-Leffler function models relaxation. Metzler and Klafter [28] explain the Mittag-Leffler function established a compromise between two apparently conflicting complexity schools, the advocates of inverse power laws and the advocates of stretched exponential relaxation, see also West *et al.* [34]. We denote with  $\Psi(t)$  the survival probability, *i.e.*, the probability that no event occurs up to time  $t$ , and we assign to its Laplace transform,  $\hat{\Psi}(u)$ , the following form (we adopt the notation for the Laplace transform  $\hat{f}(u) = \int_0^\infty d\tau \exp(-u\tau) f(\tau)$ )

$$\hat{\Psi}(u) = \frac{1}{u + \lambda^\alpha (u + \Gamma_t)^{1-\alpha}}, \quad (1.28)$$

with  $\alpha < 1$ . In the case  $\Gamma_t = 0$  this is the Laplace transform of the Mittag-Leffler function [28], a generalization of the ordinary exponential relaxation which interpolates between the stretched exponential relaxation  $\exp(-(\lambda t)^\alpha)$ , for  $t < 1/\lambda$  and the inverse power law behavior  $1/t^\alpha$ , for  $t > 1/\lambda$ .

Recent work [29] has revealed the existence of quakes within the human brain, and proved that the time interval between two consecutive quakes is well described by a survival probability  $\Psi(t)$ , whose Laplace transform fits very well the prescription of Eq. (1.28). The parameter  $\Gamma_t > 0$  has been introduced [29, 30] to take into account the truncation thought to be a natural consequence of the finite size of the time series under study. As a matter of fact, when  $1/\lambda$  is of the order of the time step and  $1/\Gamma_t$  is much larger than the unit time step, the survival probability turns out to be virtually an inverse power law, whereas when  $1/\lambda$  is of the order of  $1/\Gamma_t$  and both are much larger than the unit time step, the survival probability turns out to be a stretched exponential function.

Failli *et al.* [30] illustrate the effect of establishing a cooperative interaction in the case of the random growth of surfaces. A growing surface is a set of growing columns whose height increases linearly in time with fluctuations that, in the absence of cooperation, would be of Poisson type. The effect of cooperative

interaction is to turn the Poisson fluctuations into complex fluctuations, the interval between two consecutive crossings of the mean value being described by an inverse power law waiting time distribution  $\psi(t)$ , corresponding to a survival probability  $\Psi(t)$ , whose Laplace transform is given by Eq. (1.28). In conclusion, according to the earlier work [30], we interpret  $\alpha < 1$  as a manifestation of the cooperative nature of the process.

In this Section we illustrate a neural model where the time interval between two consecutive firings, in the absence of cooperation is described by an ordinary exponential function, thereby corresponding to  $\alpha = 1$ . The effect of cooperation is to make  $\alpha$  decrease in a monotonic way, when increasing the cooperation strength,  $K$ , with no special critical value.

We note that Barabasi [31] stressed the emergence of the inverse power law behavior, properly truncated, as a consequence of the cooperative nature of human actions. Here we interpret the emergence of the Mittag-Leffler function structure as an effect of the cooperation between neurons. The emergence of a stretched exponential function confirms this interpretation, if we adopt an intuitive explanation of it based on the distinction between the attempt to cooperate and to succeed. The action generator is assumed to not be fully successful, and a success rate parameter  $P_S < 1$  is introduced with the limiting condition  $P_S = 1$  corresponding to full success. To turn this perspective into a theory, yielding the theoretical prediction of Eq. (1.28), we assume that the time interval between two consecutive cooperative actions is described by the function  $\psi^{(S)}(\tau)$ , where the superscript ( $S$ ) indicates that from a formal point of view we realize a process corresponding to subordination theory [32, 33]. Here we make the assumption that the survival probability for an action, namely the probability that no action occurs up to a time  $t$  after an earlier action has the form:

$$\Psi^{(S)}(t) = \left( \frac{T_S}{t + T_S} \right)^\alpha, \quad (1.29)$$

with

$$\alpha = \mu_S - 1 \quad (1.30)$$

and

$$\mu_S < 2. \quad (1.31)$$

As a consequence, the time interval between two consecutive actions has the distribution density  $\psi^{(S)}(t)$  of the form

$$\psi^{(S)}(\tau) = (\mu_S - 1) \frac{T_S^{\mu_S - 1}}{(\tau + T_S)^{\mu_S}}. \quad (1.32)$$

Note that the distance between two actions is assumed to depart from the condition of ordinary ergodic statistical mechanics. In fact, the mean time distance  $\tau$  between two consecutive actions emerging from the distribution density of Eq. (1.32), is

$$\langle \tau \rangle = \frac{T_S}{\mu_S - 2}, \quad (1.33)$$

for  $\mu_S > 2$  and diverges for  $\mu_S \leq 2$ . As a consequence this process shares the same non-ergodic properties as those generated by human action [31].

It is evident that when  $P_S = 1$  the survival probability  $\Psi(\tau)$  is equal to  $\Psi^{(S)}(\tau) = \int_{\tau}^{\infty} \psi^{(S)}(\tau') d\tau'$ . When,  $P_S < 1$ , using the formalism of the subordination approach [32, 30, 29], we easily prove that the Laplace transform of  $\Psi(\tau)$  is given by

$$\hat{\Psi}(u) = \frac{1}{u + P_S \hat{\Phi}(u)}, \quad (1.34)$$

where

$$\hat{\Phi}(u) = \frac{u \hat{\psi}^{(S)}(u)}{1 - \hat{\psi}^{(S)}(u)}. \quad (1.35)$$

To prove the emergence of the Mittag-Leffler function of Eq. (1.28), with  $\Gamma_t = 0$ , from this approach let us consider for simplicity's sake the case where  $\psi^{(S)}(\tau)$  is not truncated. In the non-ergodic case  $\mu_S < 2$ , using the Laplace transform method [34], we obtain that the limiting condition  $u \rightarrow 0$  yields Eq. (1.28) with

$$\lambda = \left[ \frac{P_S}{T_S^\alpha \Gamma(1 - \alpha)} \right]^{1/\alpha}, \quad (1.36)$$

where  $\Gamma(1 - \alpha)$  is the Gamma function. Note that when  $P_S = 1$ , the Laplace transform of Eq. (1.34) in the limit of  $u \rightarrow 0$  coincides, as it must, with the Laplace transform of  $\Psi^{(S)}(t)$ . In conclusion, we obtain

$$\hat{\Psi}(u) = \frac{1}{u + \lambda^\alpha u^{1-\alpha}}, \quad (1.37)$$

with

$$\lambda^\alpha \propto P_S. \quad (1.38)$$

In the neural model illustrated hereby, we define a parameter of cooperation effort, denoted, as in the DMM case, by the symbol  $K$ . The success of cooperation effort is measured by the quantity

$$g(K) = \lambda(K)^{\alpha(K)}. \quad (1.39)$$

We determine that the sign of success is given by the number of neurons firing at the same time. We speculate that there is a connection with the dragon kings [35, 36] and coherence potentials [6].

### 1.3.2

#### Cooperation effort in a fire and integrate neural model

The NFC model refers to the interaction between  $N$  neurons, each of which has a time evolution described by

$$x(t+1) = (1 - \gamma)x(t) + S + \sigma\xi(t), \quad (1.40)$$

where  $t$  is a natural number,  $\xi(t)$  is a variable getting either the value of 1 or of  $-1$ , with equal probability, with no memory of the earlier values, and  $\gamma \ll 1$  so as to make the integer time virtually continuous when  $\gamma t \approx 1$ . The quantity  $\sigma$  is the noise intensity. The quantity  $S > 0$  serves the purpose of making the potential  $x$  essentially increase as a function of time. The neuron potential  $x$  moves from the initial condition  $x = 0$ , and through fluctuations around the deterministic time evolution corresponding to the exact solution of the case  $\sigma = 0$  [37] reaches the threshold value  $x = 1$ . When the threshold is reached it fires and resets back to the initial value  $x = 0$ . It is straightforward to prove that the variable  $x$  can reach the threshold only when the condition

$$\frac{S}{\gamma} > 1 \quad (1.41)$$

applies. In this case the time necessary for the neuron to reach the threshold, called  $T_P$ , is given by

$$T_P = \frac{1}{\gamma} \ln \left( \frac{1}{1 - \frac{\gamma}{S}} \right). \quad (1.42)$$

In the absence of interaction, the motion of each neuron is periodic, and the interval between two consecutive firings of the same neuron is given by  $T_P$ . The real sequence of firings looks random, as a consequence of the assumption that the initial conditions of  $N$  neurons are selected randomly. In this case the success rate  $g$  is determined by the random distribution of initial conditions and can be very small, as we subsequently show.

The cooperative properties of the networks are determined as follows. Each neuron is the node of a network and interacts with all the other nodes linked to it. When a neuron fires all the neurons linked to it make an abrupt step ahead of intensity  $K$ . This is the cooperation parameter, or intensity strength. An inhibition link is introduced by assuming that when one neuron fires all the other neurons linked to it through inhibition links make an abrupt step backward.

This model is richly structured and may allow us to study a variety of interesting conditions. There is widespread conviction that the efficiency of a network, namely its capacity to establish global cooperative effects, depends on network topology, as suggested by the brain behavior [29, 38]. The link distribution itself, rather than being fixed in time, may change according to the Hebbian learning principle [39]. It is expected [39] that such learning generates a scale-free distribution, thereby shedding light on the interesting issue of burst leaders [40].

All these properties are studied elsewhere. In this chapter we focus on cooperation by assuming that all the links are excitatory. To further emphasize the role of cooperation we should make the *all-to-all* (ATA) assumption adopted by Mirollo and Strogatz [37]. This assumption was also made in earlier work [41]. In spite of the fact that the efficiency of the ATA model is reduced by the action of the stochastic force  $\xi(t)$  that weakens the action of cooperation, thereby generating time complexity, the ATA condition generates the maximal efficiency and

neuronal avalanches. However, this condition inhibits the realization of an important aspect of cooperation, namely, locality breakdown. For this reason in addition to the ATA condition, we also study the case of a regular, two-dimensional (2D) network, where each node has four nearest neighbors and consequently four links. It is important to stress that to make our model as realistic as possible, we should introduce a delay time between the firing of a neuron and the abrupt step ahead of all its nearest neighbors. This delay should be assumed to be proportional to the Euclidean distance between the two neurons, and it is expected to be a property of great importance to prove the breakdown of locality when the scale-free condition is adopted. The two simplified conditions studied in this chapter, ATA and 2D, would not be affected by a time delay that should be the same for all the links. For this reason, we do not further consider time delay.

For the cooperation strength we must assume the condition

$$K \ll 1. \quad (1.43)$$

When  $K$  is of the order of magnitude of the potential threshold  $V_T = 1$ , the collective nature of cooperation is lost because the firing of a few neurons causes an abrupt cascade in which all the other neurons fire. Thus, we do not consider to be important the non-monotonic behavior of network efficiency that our numerical calculations show to emerge by assigning  $K$  values of the same order as the potential threshold.

We also note that in the case of this model the breakdown of the Mittag-Leffler structure, at large times, is not caused by a lack of cooperation, but by the excess of cooperation. To shed light on this fact, keep in mind that this model has been solved exactly by Mirollo and Strogatz when  $\sigma = 0$  [37]. In this case, even if we adopt initial random conditions, after a few steps, all the neurons fire at the same time, and the time distance between two consecutive firings is given by  $T_P$  of Eq. (1.42). As an effect of noise the neurons can also fire at times  $t \ll T_P$ , and consequently, setting  $\sigma > 0$ , a new, and much shorter time scale is generated. When we refer to this as the time scale of interest, the Mirollo and Strogatz time  $T_P$  plays the role of a truncation time and

$$\Gamma_t \approx \frac{1}{T_P}. \quad (1.44)$$

To examine this condition let us assign to  $K$  a value very close to  $K = 0$ . In this case even if we assign to all the neurons the same initial condition,  $x = 0$ , due to the presence of stochastic fluctuations the neurons fire at different times thereby creating a spreading on the initial condition that tends to increase in time, even if initially the firing occurs mainly at times  $t = nT_P$ . The network eventually reaches a stationary condition with a constant firing rate  $G$  given by

$$G = \frac{N}{\langle \tau \rangle}, \quad (1.45)$$

where  $\langle \tau \rangle$  denotes the mean time between two consecutive firings of the same neuron. For  $\sigma \ll 1$ ,  $\langle \tau \rangle = T_{MS}$ . From the condition of a constant rate  $G$  we

immediately derive the Poisson waiting time distribution

$$\psi(\tau) = \text{Gexp}(-G\tau). \quad (1.46)$$

Consequently, this heuristic argument agrees very well with numerical results.

We consider a set of  $N$  identical neurons, each of which obey Eq. (1.40) and we also assume, with Mirollo and Strogatz [37], that the neurons cooperate. For the numerical simulation we select the condition

$$G \ll 1 \ll N \ll T_P. \quad (1.47)$$

As a consequence of this choice we obtain

$$\frac{1}{G} \approx \frac{T_P}{N} \ll T_P, \quad (1.48)$$

thereby realizing the earlier mentioned time scale separation. It is evident that this condition of non-interacting neuron fits Eq. (1.28) with  $\alpha = 1$  and

$$\lambda(K = 0) = G. \quad (1.49)$$

In this case, the time truncation is not perceived, due to the condition  $1/G \ll T_P$ .

In Fig. 1.4 we show that the 2D condition is essentially equivalent to the ATA condition, provided that the cooperation strength is assumed to be an order of magnitude larger than that of the ATA condition. This is an important result, because in the case of a two-dimensional regular lattice, even though the neurons interact only with their nearest neighbors, the entire network generates the same sequence of bursts as in the ATA condition, provided that  $K$  is an order of magnitude larger. This is an indication of the fact that when the critical values of  $K$  are used two neurons become closely correlated regardless of the Euclidean length of their link, a clear manifestation of locality breakdown.

As far as the Mittag-Leffler time complexity is concerned, we adopt the same fitting procedure as that used in Ref. [41]. We evaluate the Laplace transform of the experimental  $\Psi(t)$  and use as a fitting formula Eq. (1.28) with  $\Gamma_t = 0$ , to find the parameter  $\alpha$ . Then we fit the short-time region with the stretched exponential

$$\Psi(t) = \text{exp}(-(\lambda t)^\alpha) \quad (1.50)$$

to find  $\lambda$ . We determine that in the 2D condition as in the ATA condition, switching on cooperation has the effect of generating the Mittag-Leffler time complexity. From Fig. 1.5 we see that any non-vanishing value of  $K$  turns the Poisson condition  $\alpha = 1$  into the Mittag-Leffler temporal complexity  $\alpha < 1$ . The only remarkable difference is that in the case of large cooperation strength, the value of  $\alpha$  tends to the limiting value of 0.2, whereas the ATA condition brings it to the limiting value of 0.6. The statistical analysis of data from real experiments may use this property to assess the topology of the neural network. It is expected, in fact, that all network topologies generate the Mittag-Leffler time complexity, but the actual

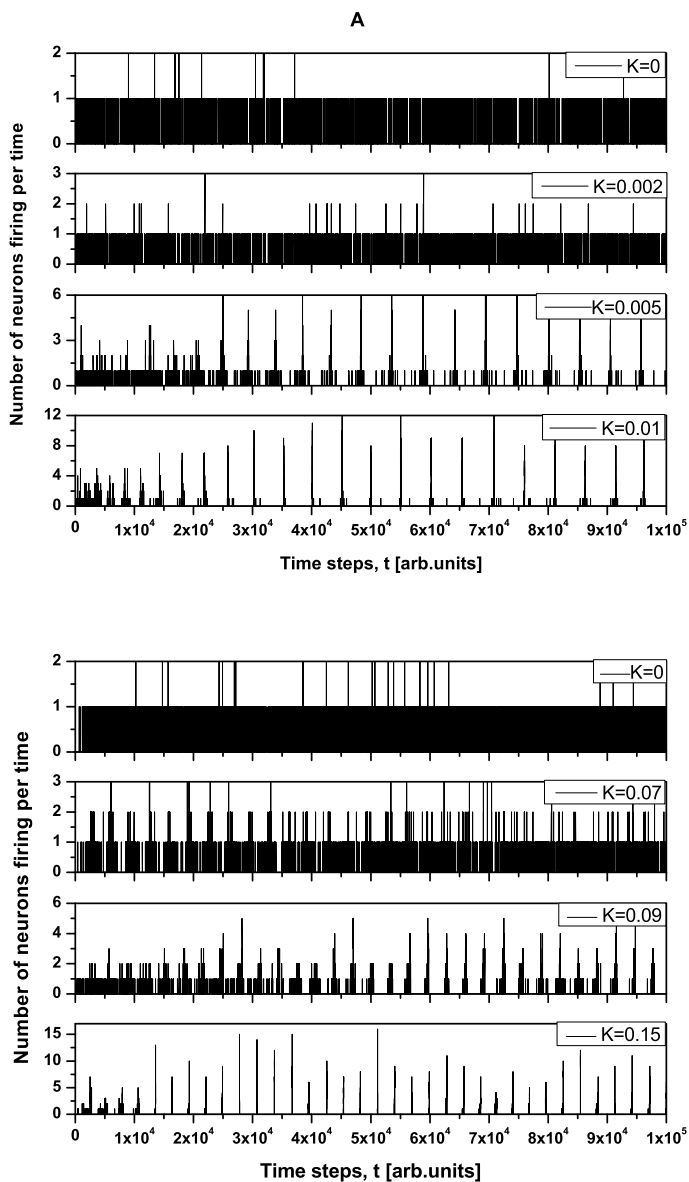


**Figure 1.4** The number of neurons firing per unit of time in the ATA (A) and 2D (B) conditions for  $K$  ranging from no cooperation to a high level. When increasing the value of  $K$  the system immediately departs from a Poisson process at  $K = 0$  to display complex cooperative behavior that then becomes strongly periodic for  $K$  large. The 2D condition shares the behavior of the ATA condition, only requiring more cooperation.



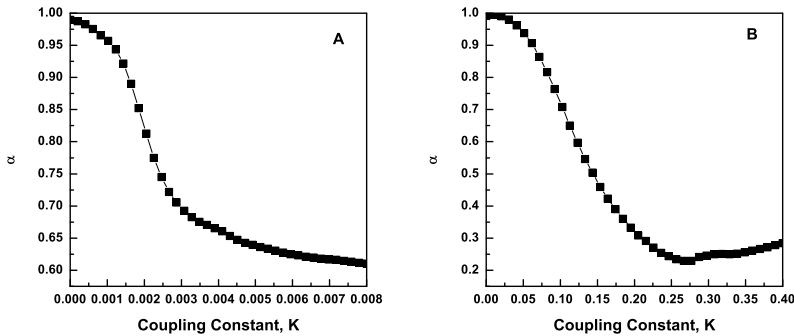


**Figure 1.5** The value of the Mittag-Leffler parameter  $\alpha$  for different cooperation levels in the ATA (A) and 2D (B) conditions. For any nonzero  $K$ ,  $\alpha < 1$ , signifying Mittag-Leffler temporal complexity.

value of  $\alpha$  depends on the network topology. Thus, the joint use of theory and experiment may further our understanding of the neural network structure.

It is interesting to notice that Fig. 1.6, in accordance with our expectation, see Eq. (1.39), shows that the success rate undergoes a significant increase at the value of the cooperation parameter  $K$  at which a distinctly Mittag-Leffler survival probability emerges.

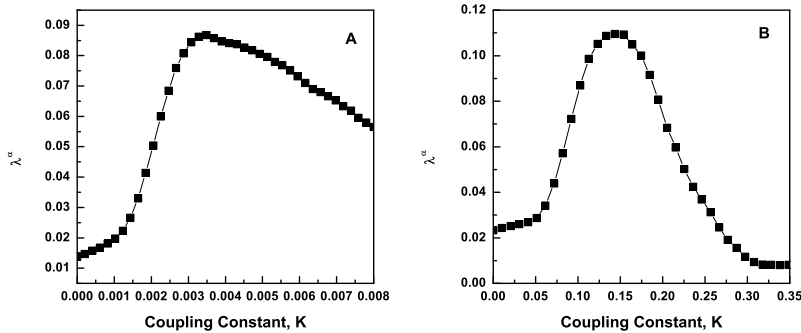


**Figure 1.6** The value of the Mittag-Leffler parameter  $\lambda^\alpha$  for different cooperation levels in the ATA (A) and 2D (B) conditions. In both cases the success rate significantly increases at the values of the cooperation strength making  $\Psi(t)$  depart from the condition of stretched exponential relaxation.

## 1.4 Avalanches and Entrainment

Neurophysiology is a field of research making significant contributions to the progress of the Science of Complexity. Sornette and Ouillon [35], who are proposing the new concept of dragon kings to go beyond the power law statistics shared by physical, natural, economic and social sciences, consider the neural avalanches found by Plenz [17] to be a form of extreme events that are not confined to neurophysiology and may show up also at the geophysical and economical level. The increasing interest in *neural avalanches* is connected to an effort to find a proper theoretical foundation, for which self-organized criticality [42] is a popular candidate, in spite of a lack of a self-contained theoretical derivation.

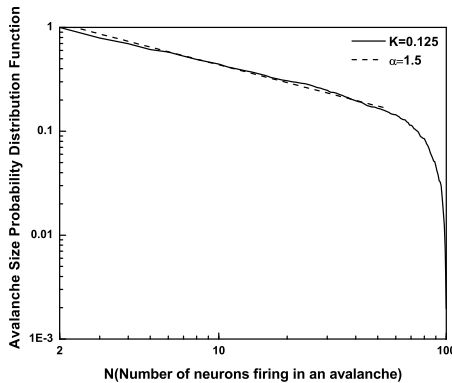


**Figure 1.7** The avalanche size distribution in the 2D condition with cooperation  $K = 0.125$ . The slope of the distribution is given by the power index  $\alpha = 1.5$ .

On the other hand, neurophysiology is challenging theoreticians with the well known phenomenon of *neural entrainment*. At first sight, the phenomenon of neural entrainment, interpreted as the synchronization of the dynamics of a set of neurons with an external periodic signal, may be thought to find an exhaustive theoretical foundation in the field of chaos synchronization [43]. This latter phenomenon has attracted the attention of many scientists in the last 22 years since the pioneering paper by Pecora and Carroll [44]. However, this form of synchronization seems to be far beyond the popular chaos synchronization. According to the authors of Ref. [45] the auditory cortex neurons, under the influence of a periodic external signal, are entrained with the stimulus in such a way as to be in the excitatory phase when the stimulus arrives, in order to process it in the most efficient way [45]. The work of neurophysiologists [46] is, on the one hand, a challenge for physicists because the experimental observation should force them to go beyond the conventional theoretical perspective of coupled oscillators, combining regular oscillations with irregular network activity while establishing a close connection

with the ambitious issue of cognition [47]. Setting aside the latter we can limit ourselves to noticing with Gross and Kowalski [4] that the entrainment between different channels of the same networks is due to excitatory synapses and consequently to neuron cooperation, rather than to the behavior of single neurons that never respond in the same way to the same stimulus.

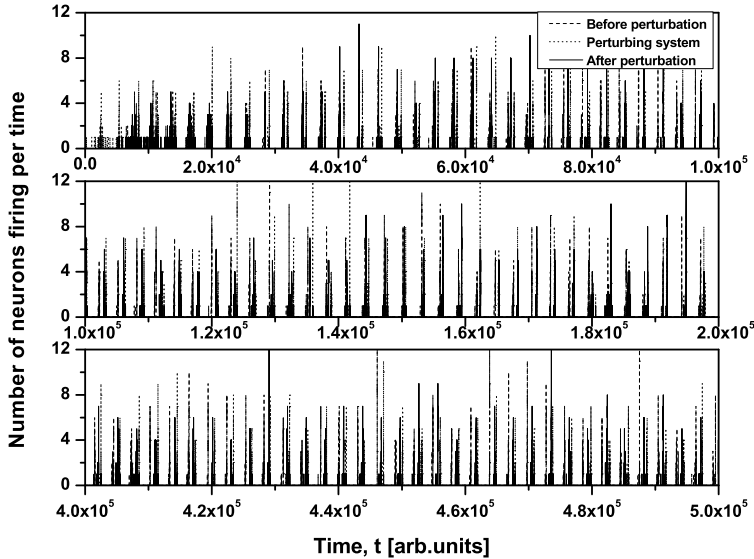


**Figure 1.8** The entrainment of the 2D neural network  $S$  (dashed lines) to an identical neural network  $P$  (dotted lines) through the forced perturbation of 3% of the nodes of  $S$ . The avalanches of the perturbed network  $S$  (solid lines) become synchronized to the perturbing network  $P$ .

Neural entrainment, on the contrary, is a global property of the whole network that is expected to generate the same response to the same stimulus. In this sense, it has a close similarity with the phenomenon of chaos synchronization, insofar as entrainment is a property of a single realization. The phenomenon of complexity management [25], on the other hand, requires averages over many responses to the same stimulus to make evident the correlation that an experimentalist may realize between response and stimulus, after designing the stimulus so as to match the complexity of the system.

Our theoretical model generates both avalanches and entrainment, thereby making clear that the phenomenon of neural entrainment is quite different from that of chaos synchronization, in spite of the fact that it shares with the latter the attractive property of being evident at the level of single realizations. Fig. 1.7 depicts an avalanche, with the typical power index of  $\alpha = 1.5$  generated by the theoretical

model of this chapter, in the case of a two-dimensional regular lattice, with  $K = 0.125$ , a strong cooperation value, corresponding to the realization of a sequence of well defined bursts, as illustrated in Fig. 1.4.

As a phenomenon of entrainment we have in mind that of the pioneering work of Ref. [19]. These authors generated a condition of maximal cooperation by chemically killing the inhibitory links, and using as a stimulus a periodic electrical stimulation. The entrainment of two 2D neural network models is shown in Fig. 1.8. Here we replace the periodic external stimulation with a neural network  $P$  identical to the perturbed neural network  $S$ . In addition, we assume that only 3% of the nodes of  $S$  are forced to fire at the same time as the neurons of the network  $P$ . This is a condition similar to that adopted elsewhere [26], with the 3% of nodes of  $S$  playing the same roles as the lookout birds [26]. These “look out” neurons are also similar to the committed minorities [3] used to realize the phenomenon of cooperation-induced synchronization.

## 1.5

### Concluding Remarks

There is a close connection between avalanches and neural entrainment. Criticality plays an important role to establish this connection, because, as well known in the field of phase transition, at criticality, as an effect of long-range correlation the limiting condition of local interaction is lost, and an efficient interaction between units that would not be correlated in the absence of cooperative interaction, is established. This condition is confined to criticality thereby implying that “intelligent” systems operate at criticality. Quite surprisingly, the model of neural dynamics illustrated in this chapter generates long-range interactions, so as to realize entrainment, for a wide range of values of  $K$ . This seems to be the extended criticality advocated by Longo and co-workers [8].

What’s the relation between these properties and the emergence of consciousness that, according to Werner [10] must be founded on renormalization group theory (RGT)? A theory as rigorous as RGT should be extended to the form of criticality advocated by Longo and co-workers [8], and this may be a difficult issue making it more challenging, but not impossible, to realize the attractive goal of Werner [10]. Werner found very promising to move along the lines outlined by Allegrini and co-workers [21] with their discovery that an intermittent behavior similar to that of Fig. 1.2, with  $\mu = 2$  may reflect cognition.

A promising, but quite preliminary result, is that of Ref. [20]. Making the assumption that cognition enters into play, with the capability of making choices generated by the intelligent observation of the decision made by the whole system, and moving along the lines that led us to Eq. (1.17), the authors of Ref. [20] found the following equation

$$\frac{d}{dt}x = -\frac{\gamma}{x} + f(t), \quad (1.51)$$

which generates an intermittent process with  $\mu = 2$ , as illustrated in Ref. [20]. We think that this results suggests two possible roads, both worthy of investigation.

The first way to realize this ambitious purpose is based on a model similar to the DMM. The units cooperate through a structure similar to that of Eqs. (1.1-1.4). A given unit may make its decision on the basis of the history of the units linked to it rather than on their state at the time at which it makes its decision. This may be a dramatic change with the effect of generating complexity for an extended range of the control parameter.

The second way is based on a model similar to the NFC model, namely the cooperative neuron model, where each unit, in the absence of cooperation, is driven by Eq. (1.40). In this model each unit has a time evolution that depends on the earlier history of the units linked to it, thereby fitting the key condition of earlier work [20]. To proceed along these lines we should settle a still open problem. The condition  $\alpha = 1$ , where the Mittag-Leffler function obtained from the inverse Laplace transform of Eq. (1.37) becomes an ordinary exponential function, is a singularity where the waiting time distribution density  $\psi(t)$ , with index  $\mu = 2$ , may be abruptly replaced by a fast decaying function, an inverse power law with index  $\mu > 2$ , and, in principle, also by an exponential function. From an intuitive point of view, this weird condition may be realized by curves of the type of those of Fig. 1.5, with the parameter  $\alpha = 1$  ( $\mu = 2$ ) remaining unchanged for an extended range of  $K$  values. In other words,  $[(d/dK)\alpha(K)]_{K=0} = 0$ . It is important to notice that the statistical analysis made by the authors of Ref. [48] to associate cognition with  $\mu = 2$  is based on observing the Rapid Transition Processes (RTP) occurring in EEG monitoring different brain areas. These authors define the simultaneous occurrence of two or more RTP as crucial events and determined that the waiting-time distribution density  $\psi(\tau)$ , where  $\tau$  is the time interval between two consecutive crucial events, is characterized by  $\mu \approx 2$ . This suggests that the authors [48] had in mind a cooperation model similar to the NFC model of this chapter, thereby making plausible our conjectures that a connection can be established between the DMM and NFC models of this chapter and the cognition model [20].

In spite of conceptual and technical difficulties that must be surpassed to achieve the important goal of Werner [10], we share his optimistic view [12] "On account of this, self-similarity in neural organizations and dynamics poses one of the most intriguing and puzzling phenomenon, with potentially immense significance for efficient management of neural events on multiple spatial and temporal scales."



## Bibliography

- 1 Beggs, J.M. and Plenz, D. (2003) Neuronal avalanches in neocortical circuits. *J. Neurosci.*, **23**, 11167-77;
- Beggs, J.M. and Plenz, D. (2004) Neuronal avalanches are diverse and precise activity patterns that are stable for many hours in cortical slice cultures. *J. Neurosci.*, **24**, 5216-29.
- 2 Touboul, J. and Destexhe, A. (2010) Can power-law scaling and neuronal avalanches arise from stochastic dynamics? *PLoS ONE*, **5**(2), e8982; de Arcangelis, L. and Herrmann, H.J. (2012) Activity-dependent neuronal model on complex networks. *Frontiers in Physiology*, **3**, 62; Li, X. and Small, M. (2012) Neuronal avalanches of a self-organized neural network with active-neuron-dominant structure. *Chaos* **22**, 023104.
- 3 West, B.J., Turlaska, M., Grigolini, P. (2012) Complex networks: from social crises to neuronal avalanches, in *this volume*, John Wiley & Sons, Ltd.
- 4 Gross, G.W. and Kowalski, J.M. (1999) Origins of activity patterns in self-organizing neuronal networks in vitro. *Journal of Intelligent Material Systems and Structures*, **10**, 558-564.
- 5 Chialvo, D.R. (2010) Emergent complex neural dynamics. *Nature Physics*, **6**, 744-750.
- 6 Plenz, D. (2012) Neuronal avalanches and coherence potentials. *The European Physical Journal-Special Topics*, **205**, 259-301.
- 7 Stanley, H.E. (1971) *Introduction to Phase Transitions and Critical Phenomena*, Oxford University Press, New York.
- 8 Bailly, F. and Longo, G. (2011) *Mathematics and the Natural Sciences: The Physical Singularity of Life*, Imperial College Press, Singapore; Longo, G. and Montévil, M. (2012) The inert vs. the living state of matter: extended criticality, time geometry, anti-entropy - an overview. *Frontiers in Physiology*, **3**, 39.
- 9 Montroll, E.W. (1981) On the dynamics of the Ising model of cooperative phenomena. *Proc. Natl. Acad. Sci. USA*, **78**, 36-40.
- 10 Werner, G. Consciousness-related brain processes viewed in the framework of phase-space dynamics, criticality, and renormalization group. *Chaos, Solitons and Fractals*, a special issue to honor Professor Werner.
- 11 Werner, G. (2007) Metastability, criticality and phase transitions in brain and its models. *BioSystems*, **90**, 496-508.
- 12 Werner, G. (2011) Letting the brain speak for itself. *Front. Physio.*, **2**, 60.
- 13 Turlaska, M., Geneston, E., West, B.J., Allegrini, P., Grigolini, P. (2012) Cooperation-induced topological complexity: a promising road to fault tolerance and Hebbian learning. *Frontiers in Fractal Physiology*, **52**, 52.
- 14 Fraiman, D., Balenzuela, P., Foss, J., Chialvo, D.R. (2009) Ising-like dynamics in large-scale functional brain networks. *Phys. Rev. E*, **79**, 061922 (1-10).
- 15 Green, M.S. (1954) Markoff random processes and the statistical mechanics of time-dependent phenomena. II. Irreversible processes in fluids. *J. Chem. Phys.*, **22**, 398-413; Kubo, R. (1957) Statistical-mechanical theory of irreversible processes. I. General theory and simple applications to magnetic and

- conduction problems. *J. Phys. Soc. Jpn.*, **12**, 570-586.
- 16 Turalska, M., Lukovic, M., West, B.J., Grigolini, P. (2009) Complexity and synchronization. *Phys. Rev. E*, **80**, 021110 (1-12).
  - 17 Klaus, A., Yu, S., Plenz, D. (2011) Statistical analyses support power law distributions found in neuronal avalanches. *PLoS ONE*, **6**, 1.
  - 18 Gerstner, W. and Kistler, W. (2008) *Spiking Neuron Models: Single Neurons, Populations, Plasticity*, Cambridge University Press, Cambridge, 2nd edn.
  - 19 Gross, G.W., Kowalski, J., Rhoades, B.K. (2000) Spontaneous and evoked oscillations in cultured mammalian neuronal networks, in *Oscillations in Neural Systems*, (eds D.S. Levine, V.R. Brown, V.T. Shirey), Erlbaum Associates, pp. 3-30. Pertinent figure: Fig. 1.9.
  - 20 Palatella, L. and Grigolini, P. (2012) Noise-induced intermittency of a reflexive model with symmetry-induced equilibrium. *Physica A*, (in press).
  - 21 Allegrini, P., Menicucci, D., Bedini, R., Gemignani, A., Paradisi, P. (2010) Complex intermittency blurred by noise: theory and application to neural dynamics. *Phys. Rev. E*, **82**, 015103(R).
  - 22 Bianco, S., Geneston, E., Grigolini, P., Ignaccolo, M. (2008) Renewal aging as emerging property of phase synchronization. *Physica A*, **387**, 1387.
  - 23 Bianco, S., Grigolini, P., Paradisi, P. (2005) Fluorescence intermittency in blinking quantum dots: renewal or slow modulation? *J. Chem. Phys.*, **123**, 174704.
  - 24 Svenkeson, A., Bologna, M., Grigolini, P. (2012) Linear response at criticality. submitted to *Phys. Rev. E*.
  - 25 Aquino, G., Bologna, M., Grigolini, P., West, B.J. (2010) Beyond the death of linear response:  $1/f$  optimal information transport. *Phys. Rev. Lett.*, **105**, 040601.
  - 26 Vanni, F., Lukovic, M., Grigolini, P. (2011) Criticality and transmission of information in a swarm of cooperative units. *Phys. Rev. Lett.*, **107**, 078103.
  - 27 Allegrini, P., Bologna, M., Fronzoni, L., Grigolini, P., Silvestri, L. (2009) Experimental quenching of harmonic stimuli: universality of linear response theory. *Phys. Rev. Lett.*, **103**, 030602.
  - 28 Metzler, R. and Klafter, J. (2002) From stretched exponential to inverse power-law: fractional dynamics, Cole-Cole relaxation processes, and beyond. *Journal of Non-Crystalline Solids*, **305**, 81.
  - 29 Bianco, S., Ignaccolo, M., Rider, M.S., Ross, M.J., Winsor, P., Grigolini, P. (2007) Brain, music, and non-Poisson renewal processes. *Phys. Rev. E*, **75**, 061911.
  - 30 Failla, R., Ignaccolo, M., Grigolini, P., Schwettmann, A. (2004) Random growth of interfaces as a subordinated process. *Phys. Rev. E*, **70**, 010101.
  - 31 Barabási, A.-L. (2005) The origin of bursts and heavy tails in human dynamics. *Nature*, **435**, 207-211.
  - 32 Sokolov, I.M. (2000) Lévy flights from a continuous-time process. *Phys. Rev. E*, **63**, 011104; Barkai, E. and Silbey, R.J. (2000) Distribution of variances of single molecules in a disordered lattice. *J. Phys. Chem. B*, (**104**), 3866; Metzler, R. and Klafter, J. (2000) From a generalized Chapman-Kolmogorov equation to the fractional Klein-Kramers equation. *J. Phys. Chem. B*, **104**, 3851.
  - 33 Sokolov, I.M. and Klafter, J. (2005) From diffusion to anomalous diffusion: a century after Einstein's Brownian motion. *Chaos*, **15**, 026103; Gorenflo, R., Mainardi, F., Vivoli, A. (2007) Continuous time random walk and parametric subordination in fractional diffusion. *Chaos, Solitons and Fractals*, **34**, 87.
  - 34 West, B.J., Bologna, M., Grigolini, P. (2003) *Physics of Fractal Operators*, Springer-Verlag, New York.
  - 35 Sornette, D. and Ouillon, G. (2012) Dragon-kings: mechanisms, statistical methods and empirical evidence. *Eur. Phys. J. Special Topics* **205**, 1-26.
  - 36 Werner, T.R., Gubiec, T., Kutner, R., Sornette, D. (2012) Modeling of super-extreme events: an application to the hierarchical Weierstrass-Mandelbrot continuous-time random walk. *Eur. Phys. J. Special Topics*, **205**, 27-52.
  - 37 Mirolo, R.E. and Strogatz, S.H. (1990) Synchronization of pulse-coupled biological oscillators. *SIAM J. Appl. Math.*, **50**, 1645.
  - 38 Kim, B.J. (2004) Geographical coarse



- graining of complex networks. *Phys. Rev. Lett.*, **93**, 168701.
- 39 Turalska, M., Geneston, E., West, B.J., Allegrini, P., Grigolini, P. (2012) Cooperation-induced topological complexity: a promising road to fault tolerance and Hebbian learning. *Frontiers in Fractal Physiology*, **3**, 52.
- 40 Ham, M.I., Bettencourt, L. M.A., McDaniel, F.D., Gross, G.W. (2008) Spontaneous coordinated activity in cultured networks: analysis of multiple ignition sites, primary circuits, and burst phase delay distributions. *Journal of Computational Neuroscience*, **24**, 346-357.
- 41 Lovecchio, E., Allegrini, P., Geneston, E., West, B.J. (2012) From self-organized to extended criticality. *Frontiers in Fractal Physiology*, **3**, 98.
- 42 de Arcangelis, L. and Herrmann, H.J. (2012) Activity-dependent neuronal model on complex networks. *Frontiers in Physiology*, **3**, 62.
- 43 Pikovsky, A., Rosenblum, M., Kurths, I. (2003) *Synchronization: a Universal Concept in Nonlinear Sciences*, Cambridge University Press, Cambridge.
- 44 Pecora, L.M. and Carroll, T.L. (1990) Synchronization in chaotic systems. *Phys. Rev. Lett.*, **64**, 821-824.
- 45 Schroeder, C.E. and Lakatos, P. (2008) Low-frequency neuronal oscillations as instruments of sensory selection. *Trends in Neurosciences*, **32**, 9.
- 46 Wang, X.J. (2010) Neurophysiological and computational principles of cortical rhythms in cognition. *Physiol. Rev.*, **90**, 1195-1268.
- 47 Dehaene, S. and Changeux, J.P. (2011) Experimental and theoretical approaches to conscious processing. *Neuron*, **70**, 202.
- 48 Allegrini, P., Menicucci, D., Bedini, R., Fronzoni, L., Gemignani, A., Grigolini, P., West, B.J., Paradisi, P. (2009) Spontaneous brain activity as a source of ideal 1/f noise. *Phys. Rev. E*, **80**, 061914.